Early history of Neanderthals and Denisovans

Alan R. Rogers[a,1], Ryan J. Bohlender[b], and Chad D. Huff[b]

[a]Department of Anthropology, University of Utah, Salt Lake City, UT 84112; and [b]Department of Epidemiology, MD Anderson Cancer Center, Houston, TX 77030

Edited by Richard G. Klein, Stanford University, Stanford, CA, and approved July 7, 2017 (received for review April 18, 2017)

Extensive DNA sequence data have made it possible to reconstruct human evolutionary history in unprecedented detail. We introduce a method to study the past several hundred thousand years. Our results show that (*i*) the Neanderthal–Denisovan lineage declined to a small size just after separating from the modern lineage, (*ii*) Neanderthals and Denisovans separated soon thereafter, and (*iii*) the subsequent Neanderthal population was large and deeply subdivided. They also (*iv*) support previous estimates of gene flow from Neanderthals into modern Eurasians. These results suggest an archaic human diaspora early in the Middle Pleistocene.

human evolution | archaic admixture | introgression | Neanderthals | Denisovans

Around 600 kya, Europe was invaded by large-brained hominins using Acheulean stone tools (1, 2). They were probably African immigrants, because similar fossils and tools occur earlier in Africa. They have been called archaic *Homo sapiens*, *Homo heidelbergensis*, and early Neanderthals, yet they remain mysterious. They may have been ancestors of Neanderthals and modern humans (3), or ancestors of Neanderthals only (4, 5), or an evolutionary dead end. According to this last hypothesis, they were replaced later in the Middle Pleistocene by a wave of African immigrants that separated Neanderthals from modern humans and introduced the Levallois stone tool tradition to Europe (6, 7). To address this controversy, we introduce a statistical method and use it to study genetic data of Africans, Eurasians, Neanderthals, and Denisovans.

Our method extends an idea introduced by Reich et al. (8, 9). Their "ABBA-BABA" statistics infer admixture from the frequency with which derived alleles are shared by pairs of samples. As we have shown (10), these estimators have large biases when populations receive gene flow from more than one source. The magnitudes of these biases depend on the sizes and separation times of ancestral populations. Our method avoids bias by estimating these parameters simultaneously.

To accomplish this, our method uses an expanded dataset. ABBA-BABA statistics summarize allele sharing by pairs of samples. We extend this approach to include larger subsets, such as trios of samples, and to use all available subsets. This opens a rich and heretofore unused window into population history.

Nucleotide Site Patterns

Although our method can accommodate complex models, we work here with a four-population model of history (Fig. 1*A*), which has broad empirical support (11, 12). In this model, Neanderthals (N) contribute genes to Eurasians (Y) but not to Africans (X). The model allows no gene flow from Denisovans (D), for reasons explained below. Combinations of uppercase letters, such as ND, refer to the population ancestral to N and D. Lowercase letters, such as n and d, refer to individual haploid genomes sampled from these populations.

The gene tree describes how genes coalesce within the tree of populations. Fig. 1*B* illustrates one of many possible gene trees. Although closely linked nucleotide sites tend to share the same gene tree, this is not the case for sites farther apart on the chromosome, and any set of autosomal sequence data will encompass a multitude of gene trees.

The gene tree determines opportunities for allele sharing among samples. For example, a mutation on the solid red branch in Fig. 1*B* would be present in y and n but absent in x and d. We refer to this as the "yn site pattern." Similarly, a mutation on the solid blue branch would generate site pattern ynd. In a four-population model, there are 10 polymorphic site patterns, excluding singletons. We can tabulate their frequencies in sequence data and calculate their probabilities given particular population histories. Our program, legofit (described in *Section S1*), estimates parameters by fitting observed to expected frequencies. Whereas ABBA-BABA statistics use only 2 site patterns ("ABBA" and "BABA"), legofit uses all 10. This allows it to estimate additional parameters and avoid the biases discussed above.

Results

We studied site-pattern frequencies in four populations at a time: an African population (X), a Eurasian populaton (Y), Neanderthals (N), and Denisovans (D). We use the high-coverage Altai Neanderthal (14) and Denisovan (12) genomes. The modern samples are from Phase I of the 1,000-Genomes Project (15). We study two African populations, the Luhuya (LWK) of East Africa and the Yoruba (YRI) of West Africa. We also study populations from the eastern and western extremes of Eurasia: Europeans (CEU) and northern Chinese (CHB). To identify different analyses, we use abbreviations such as "LWK.CHB," which means that the African population (X) is LWK and the Eurasian population (Y) is CHB. We exclude several populations of great interest—Melanesians, the San, and Pygmies—because they would require a different model of history than that in Fig. 1.

One set of 10 site-pattern frequencies is shown in Fig. 2*A*. About 30% of the nucleotide sites in these data exhibit the xy site pattern; another 20% exhibit nd. Pattern xy is common because x and y are samples from closely related populations and therefore tend to share ancestry. Mutations in these shared

Significance

Neanderthals and Denisovans were human populations that separated from the modern lineage early in the Middle Pleistocene. Many modern humans carry DNA derived from these archaic populations by interbreeding during the Late Pleistocene. We develop a statistical method to study the early history of these archaic populations. We show that the archaic lineage was very small during the 10,000 y that followed its separation from the modern lineage. It then split into two regional populations, the Neanderthals and the Denisovans. The Neanderthal population grew large and separated into largely isolated local groups.

Author contributions: A.R.R. and C.D.H. designed research; A.R.R. and R.J.B. performed research; A.R.R. and R.J.B. analyzed data; and A.R.R. wrote the paper.

The authors declare no conflict of interest.

This article is a PNAS Direct Submission.

Freely available online through the PNAS open access option.

See Commentary on page 9761.

[1]To whom correspondence should be addressed. Email: rogers@anthro.utah.edu.

This article contains supporting information online at www.pnas.org/lookup/suppl/doi:10.1073/pnas.1706426114/-/DCSupplemental.

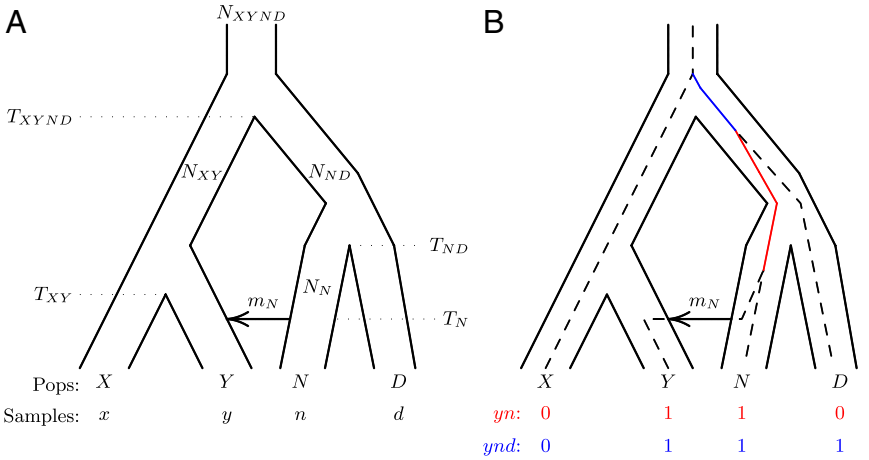

Fig. 1. (*A*) Population tree representing an African population, *X*; a Eurasian population, *Y*; Neanderthals, *N*; and Denisovans, *D*. The model involves admixture, m_N; time parameters, T_i; and population sizes, N_i. (*B*) Population tree with embedded gene tree. A mutation on the solid red branch would generate site pattern *yn* (shown in red at the base of the tree). One on the solid blue branch would generate *ynd*. Mutations on the dashed black branches would be ignored. "0" and "1" represent the ancestral and derived alleles.

ancestors generate the xy site pattern. Shared ancestry also explains the elevated frequency of nd.

As noted above, our model of history (Fig. 1*A*) excludes gene flow from Denisovans into Eurasians. This is not a limitation of our method; it is motivated by the structure of the datasets under study. To see why, consider Fig. 2*B*. Note first that yn is more common than xn—Neanderthals share more derived alleles with Europeans than with Africans. This suggests gene flow from Neanderthals into Europeans (9). More surprisingly, xd is more common than yd. The same pattern appears in all four combinations (YRI.CEU, YRI.CHB, LWK.CEU, and LWK.CHB) of African and Eurasian populations in our analysis. This pattern suggests gene flow from Denisovans into Africans, a possibility that we consider in *Section S3*. It also precludes any estimate of gene flow from Denisovans into Eurasians. For this reason, our base model includes no such term.

The analysis proceeds in two stages: one to discover dependencies among parameters and a second one imposing constraints to cope with these dependencies. In stage 1, we fit an unconstrained model to the observed data and also to 50 bootstrap replicates. With the data in Fig. 2*A*, stage 1 revealed strong dependencies among several parameters (Fig. S1). For example, there is a positive relationship between m_N, the admixture fraction, and $2N_N$, the Neanderthal population size (Fig. 3). This relationship makes sense: If the Neanderthal population were large, then most introgressing Neanderthal genes would be distantly related to the Altai Neanderthal fossil. It would therefore take more admixture to produce a given effect on the yn site pattern. On the other hand, if the Neanderthal population were small, a little admixture would have a larger effect.

Such associations make estimation difficult, because points along the regression line have similar effects on the data. To reduce such issues, stage 2 of our analysis uses associations in the bootstrap data to impose constraints. Each constraint replaces one parameter with its regression on several others, as described in *Section S1.4*. Because this involves ignoring some of the sampling variation, we do not estimate confidence intervals for constrained parameters.

To calibrate the molecular clock, we use published estimates of T_{XY} and T_{XYND}, as explained in *Section S2*. We assume a generation time of 29 y and a mutation rate of 1.1×10^{-8} per generation (16).

All four analyses—YRI.CEU, YRI.CHB, LWK.CEU, and LWK.CHB—yield similar results. Estimates of Neanderthal admixture (m_N) and Neanderthal–Denisovan separation time (T_{ND}) appear in Fig. 4. The admixture estimates are 1–3%, in broad agreement with previous results. Our results do not, however, support the view that East Asians carry more Neanderthal

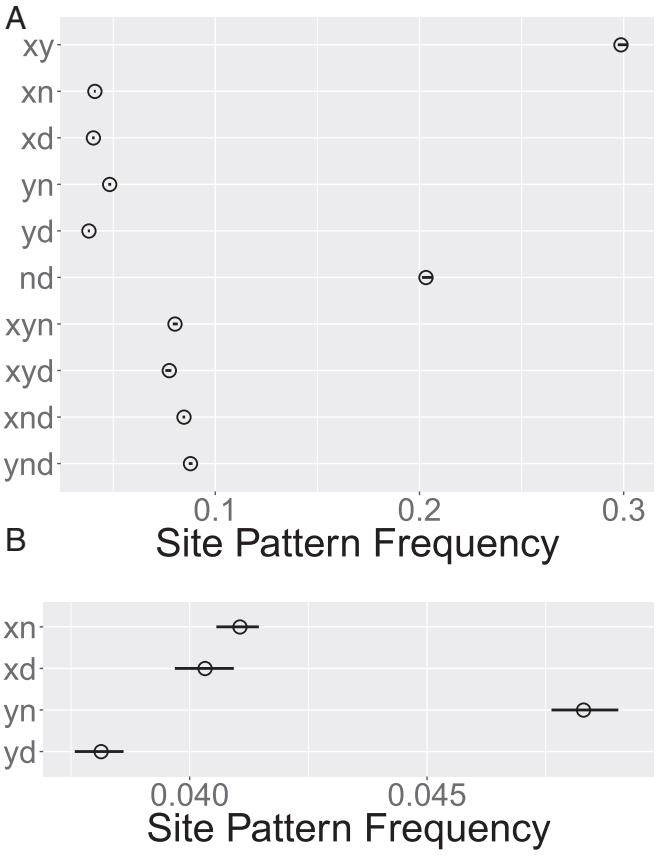

Fig. 2. (*A*) Open circles show relative frequencies (horizontal axis) of nucleotide sites exhibiting each site pattern (vertical axis) in four populations: *X*, YRI; *Y*, CEU; *N*, Neanderthal; and *D*, Denisovan. (*B*) Expanded view of four site-pattern frequencies, showing 95% confidence intervals, estimated by moving-blocks bootstrap, with 1,000 polymorphic nucleotide sites per block (13).

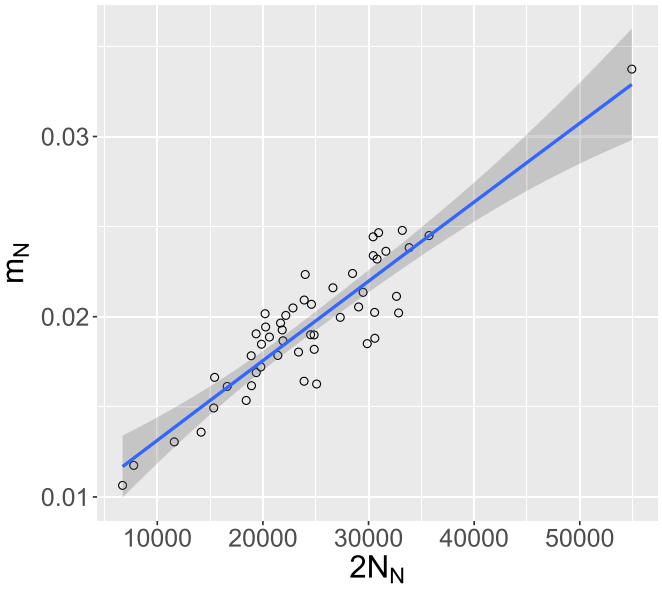

Fig. 3. Covariation of estimates of m_N and $2N_N$ across bootstrap replicates. Data are as in Fig. 2.

DNA than Europeans (12, 14, 17–21). This view may be an artifact of ascertainment bias (17) or of the biases documented by Rogers and Bohlender (10). On the other hand, the East Asian excess may be real, but hidden by the broad confidence intervals surrounding our estimates of m_N.

All estimates of T_{ND}, the separation time of Neanderthals and Denisovans, are close to 25,600 generations ago—only about 300 generations after the separation of archaics from moderns. Furthermore, this separation time is estimated with high confidence, judging from the narrow confidence intervals in Fig. 4, *Lower*. During the interval between the two separation events, the ancestral archaic population was apparently very small. Our point estimates of $2N_{ND}$ range from about 100 to about 1,000, with narrow confidence intervals. Following the Neanderthal–Denisovan separation, our results imply a relatively large Neanderthal population, with $2N$ in the tens of thousands. Fig. S3 graphs the history of effective population size of Neanderthals, moderns, and their ancestors, as implied by the YRI.CEU analysis.

Could these results be artifacts of a misspecified model? Our model (Fig. 1*A*) requires that $T_{ND} < T_{XYND}$. Yet our estimates of these parameters barely differ. Furthermore, the confidence intervals for T_{ND} are extremely—perhaps implausibly—narrow. Specification error can produce such effects by pushing all estimates, including those from bootstrap replicates, against the same boundary. The same concern also applies to the narrow confidence intervals for $2N_{ND}$, whose estimates are close to the boundary at zero.

To test this "boundary-compression" hypothesis, we used our simulation program legosim, which is described in *Section S1.5*. We simulated 50 datasets under the model implied by one set of estimates and then estimated parameters from each simulated dataset. The resulting data (Fig. 6) show how our estimator behaves in the absence of specification error. Our simulation algorithm ignores linkage disequilibrium and may therefore underestimate the widths of sampling distributions. Nonetheless, these widths are similar to those of the confidence intervals in Figs. 4 and 5, suggesting that the bias in our simulations is small. Thus, it is interesting that the spreads of T_{ND} and $2N_{ND}$ are narrow. These narrow distributions imply that we need not invoke specification error to explain the narrow confidence intervals of these parameters.

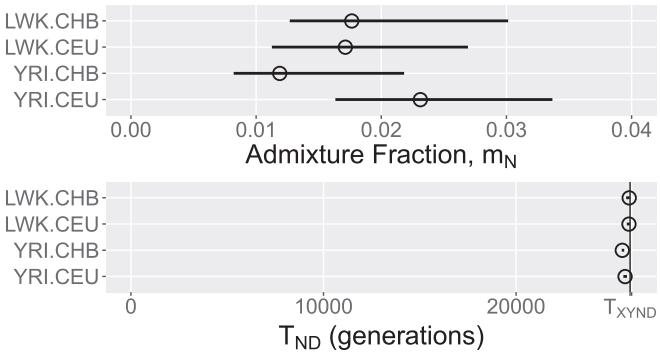

Fig. 4. Estimates of Neanderthal admixture (m_N) and the Neanderthal–Denisovan separation time (T_{ND}). The vertical line (*Lower*) shows T_{XYND}. Horizontal lines show 95% confidence intervals based on 50 moving-blocks bootstrap replicates. All point estimates and confidence intervals are based on stage 2 of the analysis.

These simulations also show that estimates of m_N and $2N_N$ are not as well behaved as those of the other parameters. They exhibit broad confidence intervals in real data (Figs. 4 and 5). In simulations (Fig. 6), they exhibit broad sampling distributions and bias. Presumably this reflects the association seen in Fig. 3. It is difficult to choose between parameter values that lie along the regression line.

Our base model (Fig. 1*A*) omits several forms of gene flow that are known or suspected, and these omissions may have

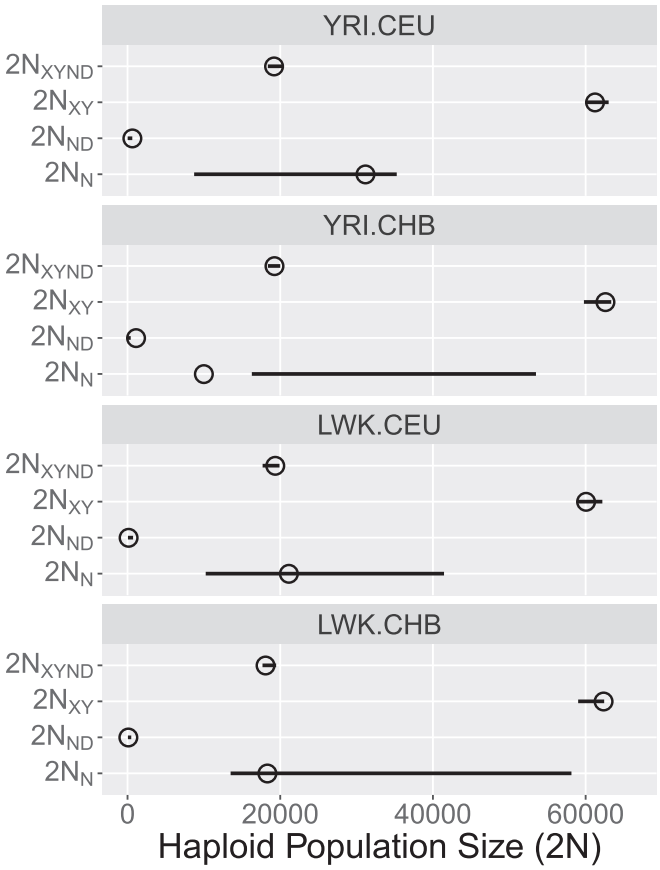

Fig. 5. Population size estimates. All point estimates are based on stage 2 of the analysis. Confidence interval for $2N_{XYND}$ is based on stage 2; other intervals are based on stage 1.

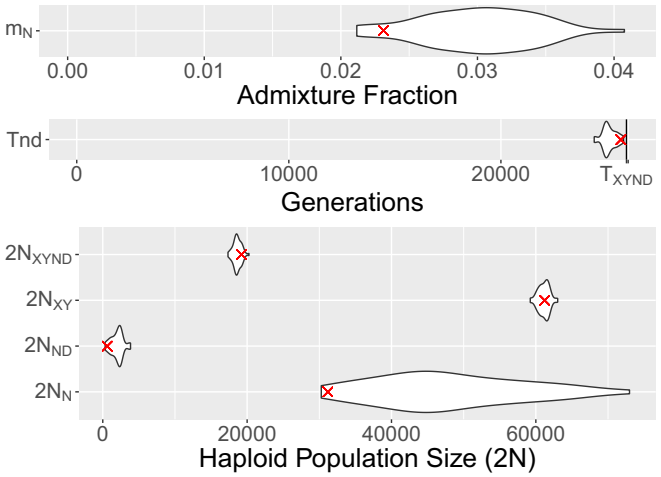

Fig. 6. Marginal sampling distributions of legofit estimates, based on 50 simulated datasets. Simulation parameters (shown as red crosses) equal the estimates from the YRI.CEU analysis in Figs. 4 and 5.

introduced bias. We therefore fitted four alternative models, as described in *Section S3*. None of these explains the surprising features of our estimates. We have found no way to explain these features as artifacts of a misspecified model.

Our estimate of the Neanderthal–Denisovan separation time is surprisingly old. The most recent whole-genome estimate of this parameter is 381 kya (ref. 14, table S12.2), which corresponds to 502 kya or 17,318 generations under our molecular clock. To determine the cause of this inconsistency, we fitted a model in which T_{ND} is fixed at 17,318 generations. The red crosses in Fig. 7 show the difference between fitted and observed site-pattern frequencies under this constrained model. The constrained model predicts too much nd but too little xnd and ynd. The predicted points lie well outside the confidence intervals. This, along with the smaller discrepancies seen elsewhere in Fig. 7, refutes the hypothesis that Neanderthals and Denisovans separated as recently as 17,318 generations ago.

Our estimate of $2N_{ND}$ is also surprising, because it implies a previously unsuspected bottleneck among the ancestors of Neanderthals and Denisovans. To explore the cause of this result, we fitted a model in which $2N_{ND}$ was constrained to equal a larger value of 10,000. The blue circles in Fig. 7 show the errors implied by this constraint. The constrained model predicts too much nd and yd but too little xnd and ynd, and many of the points lie outside the confidence intervals. The data are not consistent with a large value of $2N_{ND}$.

Our own date estimates inherit the uncertainty of the molecular clock. Using the YRI.CEU data, our point estimate of the Neanderthal–Denisovan separation time is 744 kya. Many authors prefer a higher mutation rate of 5×10^{-10} per nucleotide site per year. Under this clock, our estimate becomes 616 kya.

Discussion

These results contradict current views about Neanderthal population history. For example, Prüfer et al. (14) estimate that the Neanderthal population was very small—declining toward extinction. This view receives additional support from research showing elevated frequencies of nonsynonymous (and presumably deleterious) mutations among Neanderthals (22–24). This abundance of deleterious alleles implies that drift was strong and thus that population size was small. Yet our estimate of Neanderthal population size is large—in the tens of thousands.

To reconcile these views, we suggest that the Neanderthal population consisted of many small subpopulations, which exchanged mates only rarely. In such a population, the effective size of the global population can be large, even if each local population is small (25). A sample from a single subpopulation would show a misleading signal of gradual population decline, even if the true population were constant (26). Furthermore, there is direct evidence of large genetic differences among Neanderthal populations (22, 27). Finally, the rich and widespread fossil record of Neanderthals is hard to reconcile with the view that their global population was tiny. We suggest that previous research has documented the small size of local Neanderthal populations, whereas our own findings document the large effective size of the metapopulation that contributed genes to modern humans.

This interpretation implies that at least some of the Neanderthals who contributed to the modern gene pool were distant relatives of the Altai Neanderthal. On the other hand, there is also evidence of gene flow from moderns into the Altai Neanderthal (28). This suggests contact between modern humans and at least two groups of Neanderthals: one that was ancestral to the Altai fossil and one or more others whose relationship to Altai was distant.

As discussed above, our results also disagree with previous estimates of the Neanderthal–Denisovan separation time. On the other hand, Meyer et al. (29) show that 430 ky-old fossils from Sima de los Huesos, Spain are more closely related to Neanderthals than to Denisovans. This implies an early separation of the two archaic lineages. Our own estimate—25,660 generations, or 744 ky—is earlier still. It is consistent with the results of Meyer et al. (29) but not with those of Prüfer et al. (14), as discussed above. The cause of this discrepancy is unclear. Prüfer et al. use the pairwise sequentially Markovian coalescent (PSMC) method (30), which may give biased estimates of separation times in subdivided populations (ref. 26, p. 6).

Our results shed light on the large-brained hominins who appear in Europe early in the Middle Pleistocene. Various authors have suggested that these were African immigrants (1, 2). This story is consistent with genetic estimates of the separation time of archaics and moderns (14). Our own results imply that, by the time these hominins show up in European archaeological

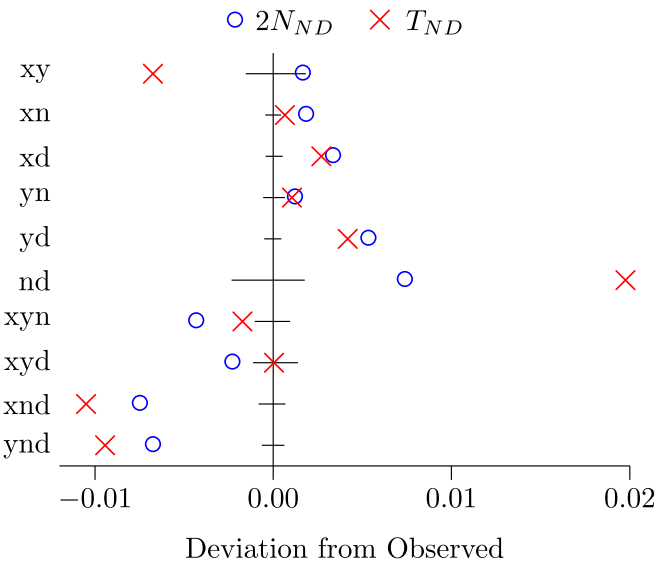

Fig. 7. Poor fit of two constrained models. Horizontal axis shows deviation of fitted from observed site-pattern frequencies under two constraints: $2N_{ND} = 10{,}000$ (blue circles) and $T_{ND} = 17{,}318$ generations (red crosses). Horizontal bars show 95% confidence intervals. Both analyses use the YRI.CEU data.

sites, they had already separated from Denisovans. This agrees with Meyer et al. (29), who show that the hominins at Sima de los Huesos were genetically more similar to Neanderthals than to Denisovans. It also agrees with Hublin (4, 5), who argues that Neanderthal features emerged gradually in Europe, over an interval that began 500–600 kya.

We estimate a small effective size in the population ancestral to Neanderthals and Denisovans. The population may have been small throughout the interval between T_{ND} and T_{XYND}, but there are also other possibilities (ref. 31, pp. 109–111). If the population varied in size, its effective size may have been much smaller than its average size. Effective size is also smaller than census size if a few individuals have disproportionate numbers of children. In a structured population, an increase in gene flow may masquerade as a reduction in effective size (26). Nonetheless, our results indicate that at least some of the time, and in at least one sex, a small number of parents produced most of the offspring.

Conclusions

It appears that Neanderthals and Denisovans separated only a few hundred generations after their ancestors left the modern lineage. During the intervening interval, the Neanderthal–Denisovan lineage was small. After separating from Denisovans, the Neanderthal population grew large and fragmented into largely isolated local groups. The Neanderthal metapopulation that contributed genes to modern humans was much larger than the local population of the Altai Neanderthal fossil.

This story is similar to that of modern Eurasians, who also separated from an African population and then experienced a population size bottleneck and split into regional populations. The modern Eurasian diaspora seems to have been foreshadowed by another one, which happened more than half a million years earlier.

Materials and Methods

Vcf files for archaic genomes were downloaded from cdna.eva.mpg.de/denisova/VCF and from cdna.eva.mpg.de/neandertal/altai/AltaiNeandertal/VCF. Ancestral-allele calls are from the Denisova genome.

We filter sites using the Map35_100% criteria (14). The minimum filtered site list was downloaded from bioinf.eva.mpg.de/altai_minimal_filters. We include only SNPs on chromosomes 1–22 that are biallelic across all samples and exclude sites in a CpG context, with systematic errors, or with missing data in any individual.

Statistical methods are described in *Sections S1* and *S2*.

ACKNOWLEDGMENTS. We are grateful for comments from Elizabeth Cashdan, Lounes Chikhi, Mitchell Lokey, Nala Rogers, Jon Seger, and Serena Tucci. A.R.R. was supported by National Science Foundation Award BCS 1638840 and by the Center for High Performance Computing at the University of Utah. R.J.B. was supported by National Cancer Institute Awards R25CA057730 (PI: Shine Chang, PhD) and CA016672 (Principal investigator: Ronald Depinho, MD). The funders had no role in study design, data collection and analysis, decision to publish, or preparation of the manuscript.

1. Klein RG (1995) Anatomy, behavior, and modern human origins. *J World Prehist* 9:167–198.
2. Klein RG (2009) *The Human Career: Human Biological and Cultural Origins* (Univ of Chicago Press, Chicago), 3rd Ed.
3. Rightmire GP (1998) Human evolution in the Middle Pleistocene: The role of Homo heidelbergensis. *Evol Anthropol Issues News Rev* 6:218–227.
4. Hublin JJ (2009) The origin of Neandertals. *Proc Natl Acad Sci USA* 106:16022–16027.
5. Hublin JJ (1998) Climatic changes, paleogeography, and the evolution of the Neandertals. *Neandertals and Modern Humans in Western Asia*, eds Akazawa T, Aoki K, Bar-Yosef O (Plenum Press, New York), pp 295–310.
6. Foley R, Lahr MM (1997) Mode 3 technologies and the evolution of modern humans. *Camb Archaeol J* 7:3–36.
7. Endicott P, Ho SYW, Stringer C (2010) Using genetic evidence to evaluate four palaeoanthropological hypotheses for the timing of Neanderthal and modern human origins. *J Hum Evol* 59:87–95.
8. Reich D, Thangaraj K, Patterson N, Price AL, Singh L (2009) Reconstructing Indian population history. *Nature* 461:489–494.
9. Green RE, et al. (2010) A draft sequence of the Neandertal genome. *Science* 328:710–722.
10. Rogers AR, Bohlender RJ (2015) Bias in estimators of archaic admixture. *Theor Popul Biol* 100:63–78.
11. Reich D, et al. (2010) Genetic history of an archaic hominin group from Denisova Cave in Siberia. *Nature* 468:1053–1060.
12. Meyer M, et al. (2012) A high-coverage genome sequence from an archaic Denisovan individual. *Science* 338:222–226.
13. Liu RY, Singh K (1992) Moving blocks jacknife and bootstrap capture weak dependence. *Exploring the "Limits" of the Bootstrap*, eds LePage R, Billard L (Wiley, New York), pp 225–248.
14. Prüfer K, et al. (2014) The complete genome sequence of a Neanderthal from the Altai mountains. *Nature* 505:43–49.
15. Abecasis GR, et al., 1000 Genomes Project Consortium (2012) An integrated map of genetic variation from 1,092 human genomes. *Nature* 491:56–65.
16. Veeramah KR, Hammer MF (2014) The impact of whole-genome sequencing on the reconstruction of human population history. *Nat Rev Genet* 15:149–162.
17. Skoglund P, Jakobsson M (2011) Archaic human ancestry in East Asia. *Proc Natl Acad Sci USA* 108:18301–18306.
18. Reich D, et al. (2011) Denisova admixture and the first modern human dispersals into Southeast Asia and Oceania. *Am J Hum Genet* 89:516–528.
19. Wall JD, et al. (2013) Higher levels of Neanderthal ancestry in East Asians than in Europeans. *Genetics* 194:199–209.
20. Sankararaman S, et al. (2014) The genomic landscape of Neanderthal ancestry in present-day humans. *Nature* 507:354–357.
21. Vernot B, Akey J (2015) Complex history of admixture between modern humans and Neandertals. *Am J Hum Genet* 96:448–453.
22. Castellano S, et al. (2014) Patterns of coding variation in the complete exomes of three Neandertals. *Proc Natl Acad Sci USA* 111:6666–6671.
23. Juric I, Aeschbacher S, Coop G (2016) The strength of selection against Neanderthal introgression. *PLoS Genet* 12:e1006340.
24. Harris K, Nielsen R (2016) The genetic cost of Neanderthal introgression. *Genetics* 203:881–891.
25. Nei M, Takahata N (1993) Effective population size, genetic diversity, and coalescence time in subdivided populations. *J Mol Evol* 37:240–244.
26. Mazet O, Rodriguez W, Grusea S, Boitard S, Chikhi L (2016) On the importance of being structured: Instantaneous coalescence rates and human evolution—Lessons for ancestral population size inference? *Heredity* 116:362–371.
27. Dalén L, et al. (2012) Partial genetic turnover in Neandertals: Continuity in the East and population replacement in the West. *Mol Biol Evol* 29:1893–1897.
28. Kuhlwilm M, et al. (2016) Ancient gene flow from early modern humans into Eastern Neanderthals. *Nature* 530:429–433.
29. Meyer M, et al. (2016) Nuclear DNA sequences from the Middle Pleistocene Sima de los Huesos hominins. *Nature* 531:504–507.
30. Li H, Durbin R (2011) Inference of human population history from individual whole-genome sequences. *Nature* 475:493–496.
31. Crow JF, Kimura M (1970) *An Introduction to Population Genetics Theory* (Harper and Row, New York).
32. Price K, Storn RM, Lampinen JA (2006) *Differential Evolution: A Practical Approach to Global Optimization* (Springer, Berlin).
33. Cleveland WS (1993) *Visualizing Data* (Hobart Press, Summit, NJ).
34. Schiffels S, Durbin R (2014) Inferring human population size and separation history from multiple genome sequences. *Nat Genet* 46:919–925.
35. Sankararaman S, Patterson N, Li H, Pääbo S, Reich D (2012) The date of interbreeding between Neandertals and modern humans. *PLoS Genet* 8:e1002947.